

Darcy's law from lattice-gas hydrodynamics

K. Balasubramanian, F. Hayot, and W. F. Saam

Department of Physics, The Ohio State University, 174 West 18th Avenue, Columbus, Ohio 43210-1106

(Received 13 April 1987)

Within the hexagonal lattice-gas model, we obtain Darcy's law for flow in the presence of scatterers. The associated momentum dissipation is described by an effective damping term in the Navier-Stokes equation, which we relate to the density of scatterers. The kinematic viscosity can be obtained from the Darcy velocity profile, once the permeability is determined. We also check that in the hexagonal lattice model, after coarse graining, velocity decay and plane-parallel Poiseuille flow occur as described by the macroscopic equations.

I. INTRODUCTION

There has been considerable recent interest in the properties of the hexagonal-lattice gas automaton,¹ viewed as a microscopic model for producing Navier-Stokes hydrodynamics. Macroscopic fluid phenomena are recovered after one defines^{1,2} average densities and velocities over suitable regions of the lattice. The description of the gas of particles moving among the sites of the lattice involves only binary arithmetic. The advantage of this approach lies in the fact that bit "democracy" is realized, complicated boundaries and shapes are easily modeled, and the algorithm can be implemented in an obvious way on parallel processor systems.

The lattice gas approach has been limited to two-dimensional phenomena.¹ It is clearly important to study *quantitatively* the connection of the hexagonal automaton to the usual approach based on the Navier-Stokes equation. The essential question is whether or not, considered as an algorithm, it can compete with those based on real number arithmetic, ordinarily used to solve those equations. Work has been done along these lines;³ much more is needed in order to answer this question.

The central result of this paper is a derivation of Darcy's⁴ law for flow in the presence of extrinsic momentum dissipation, within the context of the hexagonal lattice gas model. On the way, we check that an initial velocity distribution decays in time as expected and that, for flow between parallel plates, Poiseuille flow occurs. The parameter of physical significance in both cases is viscosity, and we check that one value is consistent with the two situations.

Darcy's law⁴ states that the velocity of the flow is proportional to the gradient of pressure

$$\mathbf{v} = -A \nabla p. \quad (1)$$

It applies to essentially two different situations, with a different physical meaning for the constant A . The first one concerns flow in porous media where $A = K/\eta$, K being defined as the permeability of the medium, and η is the viscosity of the fluid. The second one concerns experiments done in Hele-Shaw cells, where K (up to a numerical constant) is equal to the square of the distance between the parallel plates constituting the cell. One impor-

tant application of Darcy's law is in its use as the starting point of theoretical investigations of Saffman-Taylor instabilities⁵ for binary mixtures of fluids.

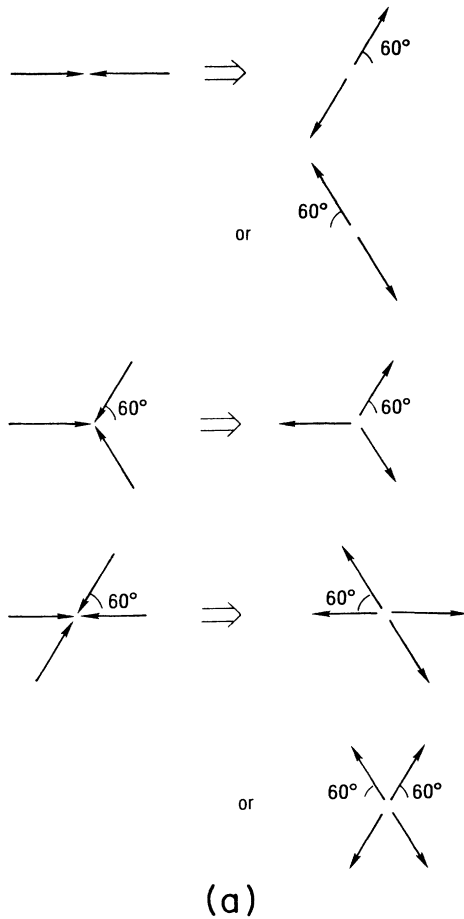
The situation modeled in the hexagonal lattice-gas automaton is the following: since Poiseuille flow is driven by a pressure gradient, we investigate how Darcy's law emerges when fixed scatterers are introduced into the flow. The scatterers provide the same type of momentum dissipation as the walls of the Hele-Shaw cell or those of the pores in a porous medium. We describe the resultant flattening of the parabolic Poiseuille velocity profile via a damping term, proportional to velocity, in the Navier-Stokes equation. We relate the coefficient of the damping term to the density of scatterers, starting from the Boltzmann transport equation for the microscopic flow of gas particles.

The model we use is the usual hexagonal lattice gas automaton.^{1,2} At each site of a two-dimensional hexagonal lattice, particles can move into any of six directions. There can be two-, three-, and four-body collisions at a site, which conserve energy and momentum. The possible collisions are shown in Fig. 1(a). The rules are such that no molecules are created, and in one time step all particles on the lattice move first to a different site, and then undergo collisions at the new site [if the configuration is one depicted in Fig. 1(a)].

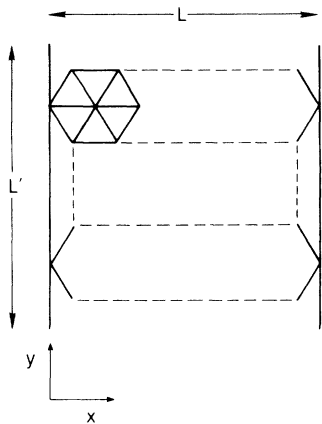
The paper is organized as follows. In Sec. II we briefly describe both the decay of an initial velocity distribution, in the absence of driving forces, and the emergence of the parabolic Poiseuille profile for plane parallel flow, both in the absence of scatterers. Section III contains our results concerning Darcy's law, and Sec. IV provides a summary and conclusions.

II. VELOCITY DECAY AND PLANE-PARALLEL POISEUILLE FLOW

The system we are considering [Fig. 1(b)] is of width $L=84$ in the x direction and length $L'=240$ in the y direction. (The lengths are expressed in terms of the link length taken to be one.) It has been previously checked⁶ that flow in this system is to a very good approximation one-dimensional, i.e., that the velocity in the y direction depends on x only, and the velocity in the x direction is



(a)



(b)

FIG. 1. (a) Collision rules for the hexagonal lattice-gas model. Examples are shown of two-body, three-body, and four-body collisions. Collisions conserve energy and momentum. (b) Sketch of the two-dimensional system studied. The longitudinal direction is the y direction, where L' is the number of sites in that direction. The transverse direction is the x direction, with L sites. The lateral boundaries consist of a succession of hexagonal sites. One complete hexagon is drawn.

negligible in comparison.

Macroscopic mean density ρ (the mass of a particle is taken to be one) and velocity \mathbf{u} are defined by

$$\rho = \frac{2}{\sqrt{3}} \frac{1}{M} \sum_{i,\alpha} (N_\alpha)_i, \tag{2}$$

$$\rho \mathbf{u} = \frac{2}{\sqrt{3}} \frac{1}{M} \sum_{i,\alpha} (N_\alpha \mathbf{c}_\alpha)_i, \tag{3}$$

where the sum over i is over the number of sites in the region considered, M is the total number of sites in that region, and the factor of $2/\sqrt{3}$ is due to the fact that for the hexagonal lattice the number of sites per unit area is $2/\sqrt{3}$ and not 1.⁷ $N_{\alpha i}$ is the number of particles at site i , moving into direction α , and $\mathbf{c}_{\alpha i}$ is the unit length velocity vector at site i , pointing into direction α ($\alpha = 1, 2, \dots, 6$).

Instead of (2) we will be using in the following discussion the quantity

$$\bar{\rho} = \frac{\sqrt{3}}{2} \frac{\rho}{6}, \tag{3'}$$

the average number of particles per link. $6\bar{\rho}$ then corresponds to the average number of particles per site. The velocity \mathbf{u} is the same for all these definitions.

Since it is the x dependence of the velocity we are interested in, a macroscopic region in our work is taken to be a longitudinal slice of lattice of length 220 and width 6 (in unit links). There are thus 14 data points in the x direction. Let us now discuss in turn velocity distribution decay and Poiseuille flow.

A. Velocity decay

Here an initial distribution of particles is introduced, with a given density, and having a net average flow in the y direction. The initially flat profile decays in time due to no-slip boundary conditions at the lateral walls (no-slip means here that any particle that hits the wall along any of three possible directions bounces back into the incoming direction). Boundary conditions at the top and bottom ends are periodic. Fluid behavior for this flow satisfies the Navier-Stokes equation

$$\frac{\partial u}{\partial t} = \nu \frac{\partial^2 u}{\partial x^2}, \tag{4}$$

where u denotes the velocity component in the y direction and $\nu = \eta/\rho$ is the kinematic viscosity.

The solution to (4) is of the form

$$u(x, t) = \sum_{m=0}^{\infty} u_m \cos(k_m x) e^{-\nu k_m^2 t},$$

where $k_m = (2m + 1)\pi/L$, L being the width of the system, and x varies between $-L/2$ and $L/2$. The velocity averaged over x is

$$\bar{u}(t) = u_0 \sum_{m=0}^{\infty} \frac{8}{\pi^2 (2m + 1)^2} \exp(-\nu k_m^2 t), \tag{5}$$

where u_0 is the initial flat velocity distribution. The kinematic viscosity is of order 1, and, as soon as t is bigger

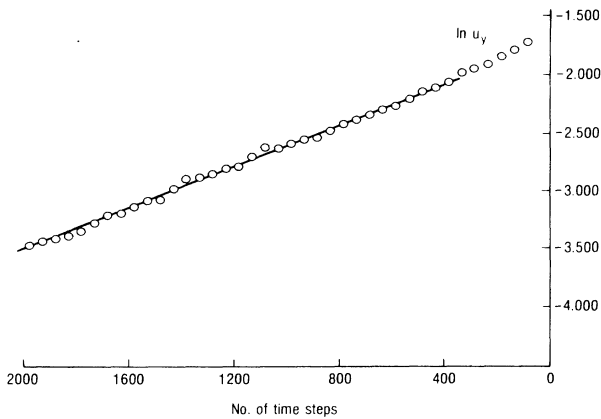


FIG. 2. Velocity decay for a uniform initial profile. Shown is the logarithm of velocity u_y as a function of the number of time steps, increasing from right to left. The experiment is done at an average number of two particles per site.

than 500, the sum in (5) is dominated by the $m = 0$ term:

$$\bar{u}(t) \approx \frac{8u_0}{\pi^2} \exp \left[-\nu \frac{\pi^2}{L^2} t \right]. \quad (6)$$

For the hexagonal lattice model, with the definition of velocity and density as given by (3) and (4), the decay of average velocity follows exactly the form (6), as shown in Fig. 2 on a plot of velocity versus time. Several runs at a density $\bar{\rho}$ of $1/3$ [cf. Eq. (3)] and for various initial uniform velocities, lead to a kinematic viscosity in the range

$$0.60 \leq \nu \leq 0.64.$$

This is to be compared with a calculated Boltzmann value of $\nu = 0.55$, which includes a correction due to the discrete nature of the system.^{7,8} We consider it satisfactory that the value obtained from velocity decay is within 10% of this value. For Poiseuille flow (see below) the value determined from the numerical experiments turns out to be $\nu = 0.63$.

It should be pointed out here that viscosity is not well defined in two dimensions.⁹ It diverges (at least in principal) logarithmically with the size of the system. The viscosity determined here should therefore be regarded as an effective one, corresponding to the system size considered. The logarithmic variation of course makes any dependence on system size very weak.

B. Plane-parallel Poiseuille flow

This case corresponds to a flow maintained by a longitudinal constant pressure gradient dp/dy . The solution to the Navier-Stokes equation

$$\eta \frac{d^2 u}{dx^2} = \frac{dp}{dy}$$

is given by the usual parabolic profile

$$u = \frac{-1}{2\eta} \frac{dp}{dy} x(L-x). \quad (7)$$

How is this situation created in the hexagonal lattice gas? For the lattice gas, pressure is proportional to density, given by $p = \frac{1}{2}\rho$.^{1,8} The density gradient from bottom to top of the system is created by randomly taking two-particle collisionless configurations on the bottom line, and turning these particles into the two up directions, thus injecting momentum into the system. Periodic boundary conditions are maintained in the propagating phase of the time step update (cf. Introduction). Lateral boundary conditions are no slip, as in Sec. II A.

Figure 3 shows that the parabolic velocity profile is obtained in the hexagonal lattice gas model.¹⁰ This corresponds, at a density $\bar{\rho}$ of $\frac{1}{3}$, to a measured density gradient $\bar{\Delta}\rho/\Delta y$ of 5.82×10^{-5} . From the average velocity given by

$$\bar{u} = -\frac{L^2}{24\nu} \frac{1}{\rho} \frac{d\rho}{dy} = -\frac{L^2}{24\nu} \frac{1}{\bar{\rho}} \frac{d\bar{\rho}}{dy} \quad (8)$$

we extract a value for ν of (for $\bar{u} = 0.081$)

$$\nu = 0.63.$$

This value is compatible with that derived above from the decay of velocity profile, and within 15% of the value calculated in the Boltzmann approximation. Equation (8) is obtained from (7) using the relationship between pressure and density $p = \rho/2$.

Numerical data are obtained by doing time averages (over several thousand time steps), once the system has reached steady state (after 6000 time steps). There is a

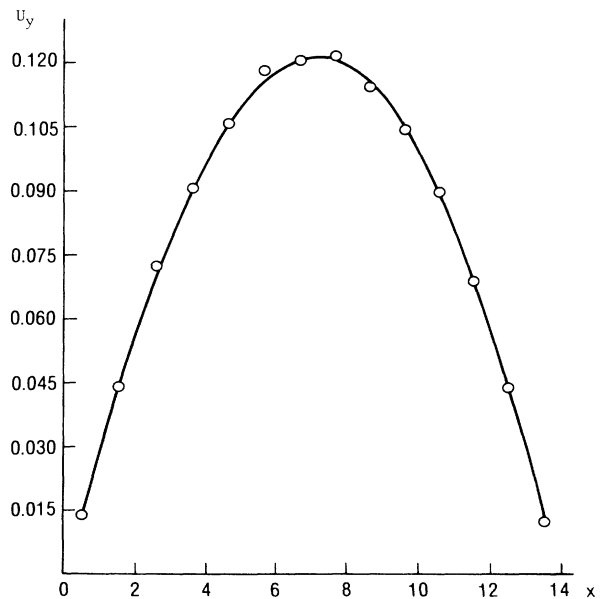


FIG. 3. Parabolic velocity profile u_y as a function of x , for Poiseuille flow. Each unit in the x direction corresponds to 6 lattice units (for details see text). The fit is obtained through a plotting routine. Here $|d\bar{\rho}/dy| = 5.82 \times 10^{-5}$, at an average number of two particles per site.

source of error here peculiar to the lattice-gas model: The pressure, and thus the density, acquires a u^2 dependence. Since u depends on x , this creates a lateral density gradient, not taken into account in the Navier-Stokes equation [Eq. (7)]. This effect is, however, small as long as the maximum velocity is small (here $u \max \simeq 0.12$).^{11,12}

The main point is that the parabolic profile is found and that the kinematic viscosity determined from it is compatible with the value found from the decay of an initially flat velocity distribution (cf. Sec. II A).

III. DARCY'S LAW

As noted in the Introduction [see Eq. (1)], Darcy's law is relevant to flow in porous media such as rocks, and in Hele-Shaw cell experiments on binary mixtures. We wish to study how this law emerges from the hexagonal lattice-gas model. This model being two and not three-dimensional, we proceed by mimicking the porosity of the medium (or effects of the walls of a Hele-Shaw cell) by introducing a small density of scatterers. These are sites in the system, where any incident particle bounces back into its incoming direction. They act as a reservoir of momentum. Their density is very low compared to that of the gas, so that the mean free path of a gas particle is essentially unaffected by their presence. If the original flow is of Poiseuille type, driven by a pressure gradient (cf. Sec. II B), the presence of the scatterers slows down the flow and flattens the profile.

Our results can be described by introducing a damping term, proportional to velocity, into the Navier-Stokes equation. (Terms of this general form are discussed in Appendix D of Ref. 13.) The coefficient α of this term is proportional to the density of scatterers and is estimated below in the Boltzmann approximation to the lattice-gas model. With the presence of a damping term, the effective Navier-Stokes equation reads

$$v \frac{d^2 u}{dx^2} - \alpha u = \frac{1}{\rho} \frac{dp}{dy}, \quad (9)$$

where α is positive, and dp/dy is the pressure gradient. We recall that pressure is proportional to density in the hexagonal lattice model (cf. Sec. II B). The solution to (9) with boundary conditions $u(0) = u(L) = 0$, is given by

$$u(x) = -\frac{1}{\alpha} \frac{1}{\rho} \frac{dp}{dy} \left[1 - \frac{\cosh[r(x-L/2)]}{\cosh(rL/2)} \right], \quad (10)$$

where $r = \sqrt{\alpha/v}$. When α goes to zero, (10) reduces to the usual parabolic velocity profile given by (7). The average velocity corresponding to (10) is

$$\bar{u} = -\frac{1}{\alpha} \frac{1}{\rho} \frac{dp}{dy} \left[1 - \frac{2}{Lr} \tanh(rL/2) \right]. \quad (11)$$

The coefficient α in (9), (10), or (11) is proportional to the density of scatterers. The coefficient of proportionality can be estimated by starting from the microscopic model, in the Boltzmann approximation, which states that, at a given site,

$$N_\alpha(t+1, \mathbf{r} + \mathbf{c}_\alpha) - N_\alpha(t, \mathbf{r}) = \Omega_\alpha, \quad (12)$$

where α is one of six directions in the hexagonal lattice model, N_α is the number of particles going into direction α , \mathbf{c}_α is the unit vector of direction α , and Ω_α is the collision term. Using definitions (2) and (3) for average density and velocity, Eq. (12) leads, after summation, to mass conservation, and, after multiplication with \mathbf{c}_α and summation, to momentum conservation. Let us concentrate in Ω_α on the part that describes the bouncing back of any particle either into or out of direction α , after hitting a scatterer at site α . The assumption of molecular chaos is of course made here. We denote by N_s the number of scatterers at given site. Then

$$\Omega_\alpha = N_s (N_{\alpha+3} - N_\alpha). \quad (13)$$

Assuming local thermodynamic equilibrium, N_α can be expanded as⁸

$$N_\alpha = \frac{\sqrt{3}}{2} \frac{\rho}{6} (1 + 2\mathbf{c}_\alpha \cdot \mathbf{u} + \dots). \quad (14)$$

[The factor of 2 in (14) is consistent with the definition of \mathbf{u} [see Eq. (3)] and the fact that $\sum_\alpha (c_\alpha)_i (c_\alpha)_j = 3\delta_{ij}$ for a two-dimensional hexagonal lattice. The assumption of local thermodynamic equilibrium here requires that the collision time τ for particle-particle collisions is short compared to the analogous time τ_I for particle-impurity collisions. In terms of the corresponding mean free paths λ and λ_I , we require $\lambda \ll \lambda_I$. As $\lambda \sim 10$, and $\lambda_I \sim 1/N_s$, we require $N_s \ll \frac{1}{10}$. The largest impurity density considered here is $N_s \approx \frac{1}{100}$.

Multiplying (12) by \mathbf{c}_α , summing over α , and using expression (14) up to second order in \mathbf{u} , leads to the Navier-Stokes equation, as described in Ref. 2. We are interested in the collision term (13), which upon performing the above operations becomes [up to an overall normalization of $(2/\sqrt{3})(1/M)$, cf. (2) or (3)]

$$\sum_\alpha \mathbf{c}_\alpha \Omega_\alpha = N_s \sum_\alpha \mathbf{c}_\alpha (N_{\alpha+3} - N_\alpha).$$

Using expression (14), this becomes

$$\begin{aligned} \sum_\alpha \mathbf{c}_\alpha \Omega_\alpha &= 2N_s \frac{\rho}{6} \frac{\sqrt{3}}{2} \sum_\alpha \mathbf{c}_\alpha [(\mathbf{c}_{\alpha+3} - \mathbf{c}_\alpha) \cdot \mathbf{u}] \\ &= -4N_s \frac{\rho}{6} \frac{\sqrt{3}}{2} \sum_\alpha \mathbf{c}_\alpha (\mathbf{c}_\alpha \cdot \mathbf{u}), \end{aligned}$$

since $\mathbf{c}_{\alpha+3} = -\mathbf{c}_\alpha$. Now $\sum_\alpha (c_\alpha)_i (c_\alpha)_j = 3\delta_{ij}$ for the hexagonal lattice and thus we have

$$\sum_\alpha \mathbf{c}_\alpha \Omega_\alpha = -2 \frac{\sqrt{3}}{2} N_s \rho \mathbf{u}. \quad (15)$$

$N_s < 1$ is simply the average number of scatterers at a site. Expression (15) leads to a damping term in the Navier-Stokes equation. Taking into account the extra factor of $(2/\sqrt{3})(1/M)$ in the normalization (see above) and the fact that in order to arrive at Eq. (9), there has been a division by the density ρ , one obtains for the coefficient of the damping term in (9) the expression

$$\alpha = 2N_s . \quad (16)$$

This relation between α and N_s depends on the form of the particle-scatterer collision term, given in expression (13).

The numerical experiments to test Darcy's law have been done with 200 scatterers, corresponding to a site density $N_s = 0.01$. The scatterers are distributed randomly among the lattice sites, and flow is driven by a density gradient as in Sec. II. In Fig. 4 we show the velocity profile, averaged over an ensemble of 20 systems, each with 200 scatterers. The velocity profile is flattened out, as expected, in comparison to that obtained in Poiseuille flow (Fig. 3). The curvature of the profile is small except near the boundaries. As a consequence the viscous term in Eq. (9) is small compared to the damping term over most of the channel, leading to Darcy's law

$$u_y(x) = -\frac{1}{\rho\alpha} \frac{dp}{dy} , \quad (17)$$

with the constant $A = 1/\rho\alpha$ in Eq. (1). The permeability K of our system is, hence,

$$K = \frac{\eta}{\rho\alpha} = \nu/\alpha = \frac{1}{r^2} , \quad (18)$$

and is proportional to the square of the healing length $1/r$ of Eq. (10).

A simple measure of the flatness of the profile is the ratio u_{\max}/\bar{u} , which, for Fig. 4, is equal to 1.2, compared to 1.5 for Poiseuille flow and 1.0 for a perfectly flat profile. Numerically, the average velocity $\bar{u} = 0.0164$ is determined directly for the data of Fig. 4. The profile shape is then fit by the single parameter $r = \sqrt{\alpha/\nu}$, with the result that $r = 0.133$.

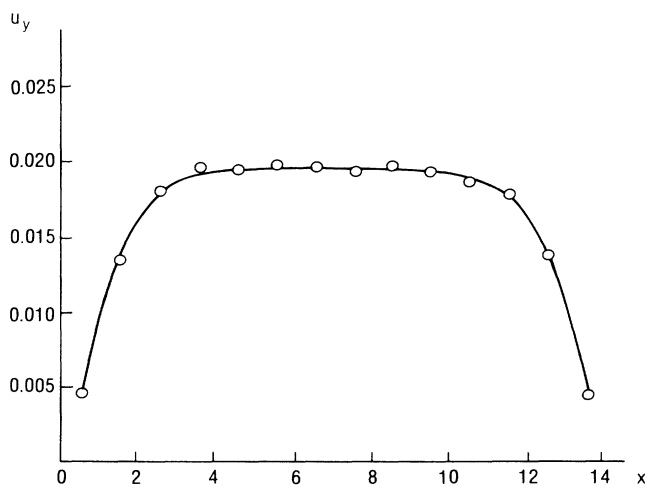


FIG. 4. Velocity profile of a pressure driven flow in the presence of scatterers. Lateral boundary conditions are no-slip and an average over systems of scatterers has been taken (for details see text).

Use of Eq. (11) with $\alpha = \nu r^2$ allows extraction of the viscosity ν from the data via

$$\nu = -\frac{1}{\bar{u}r^2} \frac{1}{\rho} \frac{\partial p}{\partial y} \left[1 - \frac{2}{rL} \tanh \left(\frac{rL}{2} \right) \right] . \quad (19)$$

As

$$\frac{1}{\rho} \frac{\partial p}{\partial y} = \frac{1}{2\rho} \frac{\partial \rho}{\partial y} = 2.34 \times 10^{-4}$$

for the data of Fig. 4, we find $\nu = 0.66$. We estimate the error on ν to be 20%. The value of ν is consistent with the values for ν found in Sec. II. Then

$$\alpha = 0.011 = 1.1N_s . \quad (20)$$

This differs from the simple Boltzmann result of Eq. (16). The assumptions of low density and molecular chaos going into the Boltzmann derivation are not really satisfied.

A further numerical experiment, yielding α directly, has been carried out as a control on our above results. The experiment uses free slip boundary conditions at the walls, resulting in a flat profile $u_y = 0.016 = \text{const}$. Directly, from Eq. (17) we obtain $\alpha = 1.17 \times 10^{-2}$ which, within our accuracy, is compatible with that given by Eq. (20). The pressure gradient here was

$$\frac{1}{\rho} \frac{d\rho}{dy} = 3.75 \times 10^{-4} .$$

Note that the density gradients quoted above correspond to a total density variation in the y -direction of 10%. All effects of compressibility, at this level, have been taken to be negligible in our work. Further reduction of the gradient is, of course, possible, but leads to noisier velocity profiles.

IV. SUMMARY AND CONCLUSION

We have studied fluid flow within the hexagonal lattice-gas model in the presence of randomly situated scatterers. Darcy's law is obtained in the limit where viscous edge effects are negligible. Additional checks on the validity of a hydrodynamics for the coarse-grained lattice-gas include driven (Poiseuille) and decaying flow between walls with no-slip boundary conditions. The results of all of these numerical experiments are consistent with one another and with the appropriate hydrodynamic description. The effective kinematic viscosity common to all phenomena is equal to 0.63 ($\pm 5\%$) at an average density of two particles per site. The lattice gas, with some restrictions,^{11,12} appears to provide an appropriate tool for the study of simple hydrodynamics phenomena. Whether it is an efficient way to study more complex phenomena, such as the Saffman-Taylor instability⁵ and turbulent flow around obstacles remains to be investigated.

- ¹U. Frisch, B. Hasslacher, and Y. Pomeau, *Phys. Rev. Lett.* **56**, 1505 (1986).
- ²J. Salem and S. Wolfram, in *Theory and Applications of Cellular Automata*, edited by S. Wolfram (World Scientific, Singapore, 1986).
- ³Proceedings of the Workshop, Modern Approaches to Large Nonlinear Physical Systems, Santa Fe, 1986, edited by G. Doolen (unpublished).
- ⁴G. K. Batchelor, *An Introduction to Fluid Dynamics* (Cambridge University Press, Cambridge, England, 1967).
- ⁵P. G. Saffman and G. Taylor, *Proc. R. Soc. London, Ser. A* **245**, 312 (1958).
- ⁶F. Hayot, *Phys. Rev. A* **35**, 1774 (1987).
- ⁷M. Henon, in Proceedings of the Workshop, Modern Approaches to Large Nonlinear Physical Systems, Ref. 3.
- ⁸U. Frisch and J. P. Rivet, *C. R. Acad. Sci. Paris II* **303**, 1065 (1986); S. Wolfram, *J. Stat. Phys.* **45**, 471 (1986).
- ⁹D. Forster, D. R. Nelson, and M. J. Stephen, *Phys. Rev. A* **16**, 732 (1977).
- ¹⁰D. d'Humieres and P. Lallemand, *C. R. Acad. Sci. Paris II* **302**, 383 (1986); *Physica* **140A**, 337 (1986).
- ¹¹J. P. Dahlburg, D. Montgomery, and G. D. Doolen (unpublished).
- ¹²F. Hayot, in Proceedings of the Workshop, Modern Approaches to Large Nonlinear Physical Systems, Ref. 3.
- ¹³U. Frisch, D. d'Humieres, B. Hasslacher, P. Lallemand, Y. Pomeau and J. P. Rivet, in Proceedings of the Workshop, Modern Approaches to Large Nonlinear Physical Systems, Ref. 3.